CFD analysis on the aerodynamic coefficients of an ejection seat system at supersonic speed

Md. Mahbubur Rahman[1*]*, Sunil Chandel*[1], and *D. G. Thakur*[1]

[1]Department of Mechanical Engineering, Defence Institute of Advanced Technology (DU), Girinagar, Pune - 411025, India

Abstract. In the present study, a 3-D study of the aerodynamic coefficients of an ejection seat system is performed. The analysis is performed using the Reynolds Averaged Navier-Stokes equations where an unstructured grid of the polyhedral cells is used. The aerodynamic coefficients are calculated using a density-based solver and the standard k-ε turbulence model. The investigation is performed at Mach number (Ma) = 1.25 by varying the angle of attack (α) from -15^0 to 15^0 with the increment of 5^0 where the yaw angle (β) is fixed at 0^0. According to the findings, the magnitude of the axial force coefficient (C_X) increases as α decreases whereas the value of the normal force coefficient (C_Z) decreases with the increase of α. Similarly, the value of the pitching moment coefficient (C_m) decreases with the increase of α.

1 Introduction

A military fighter aircraft is made up of several different sorts of equipment, one of which is the ejection seat system. This system is composed of different small components. The main objective of the system is to save the pilot's life when required. With time the ejection seat system has developed a lot. After World War II the modern aircraft was manufactured with the developed ejection seat system that protects the pilot's life from any catastrophic failure.

During the ejection of the pilot along with the ejection seat from the cockpit, the pilot is suddenly exposed to an environment where the free stream velocity of the air can be supersonic. During the ejection procedure, the pressure forces exerted on the pilot's body change as the ejection seat system rotates. The rotation of the ejection seat system is unpredictable during the process. Hence, during the analysis of an ejection seat system, many orientations of the ejection seat are to be analyzed. Initially through experimental methods [1], the ejection seat system was analyzed. However, the development of the CFD which is used in various applications [2-4] of the fluid dynamics makes it possible to analyze the ejection seat system with less time and cost.

Habchi et al. [5] performed a steady-state analysis of a 3-D ejection seat system at Ma = 0.6 and 0.9 by varying α. Initially, they analyzed a 2-D ejection seat system and later on analyzed a 3-D ejection seat system where the effect of the Ma and the effect of the variation of the α and β was analyzed. The effect of a yaw fin along with the ejection seat system was further measured by changing β. Later in 1995, Habchi and Hufford [6] studied an unsteady

---

* Corresponding author: mahbub.rizvee@gmail.com

state analysis on the ejection seat system at Ma = 0.6. Initially, a classical blunt body (cylinder) was studied for different grids. After that, a 2-D ejection seat system was analyzed before analyzing a 3-D ejection seat system.

A numerical and experimental investigation of the ejection seat was studied by Chen et al. [7] at Ma = 0.6, 0.9, and 1.2. They observed the aerodynamic coefficients by varying α and β. From their study, they concluded that the numerical and the experimental results match pretty well. Zhu et al. [8] observed the detachment of the ejection seat system from the cockpit using an overset chimera grid in CFD-FASTRAN. This analysis was performed after the validation at Ma = 0.6 which was performed by varying α and β. The importance of using a protective device along the ejection seat system was analyzed at Ma = 0.9 by Tian and Chen [9]. An unstructured grid of tetrahedron cells was solved using the Spalart-Allmaras turbulent model to analyze the aerodynamic coefficients in ANSYS-Fluent. They observed that a significant amount of axial force was reduced after the installation of a protective device with the ejection seat system.

In 2012 Zhu et al. [10] analyzed the canopy separation from the aircraft using CFD-FASTRAN. Later on, they performed an unsteady state analysis on the ejection seat system using a standard wall function to observe the detachment of the TY-5 ejection seat from the aircraft at Ma = 1.2. At Ma = 0.9, an unscaled ACES II ejection seat was evaluated to determine the aerodynamic coefficient for various values of α and β by Guan et al. [11]. They validated the numerical approach with the experimental results at Ma = 0.6. Investigation of the aerodynamic coefficients of the ejection seat assuming a steady-state condition was performed by Mahbub et al. [12]. They analyzed the ejection seat system by varying Ma, α, and β to generate a database. This investigation was performed using the standard k-ε turbulence model in ANSYS-Fluent where unstructured grids were utilized.
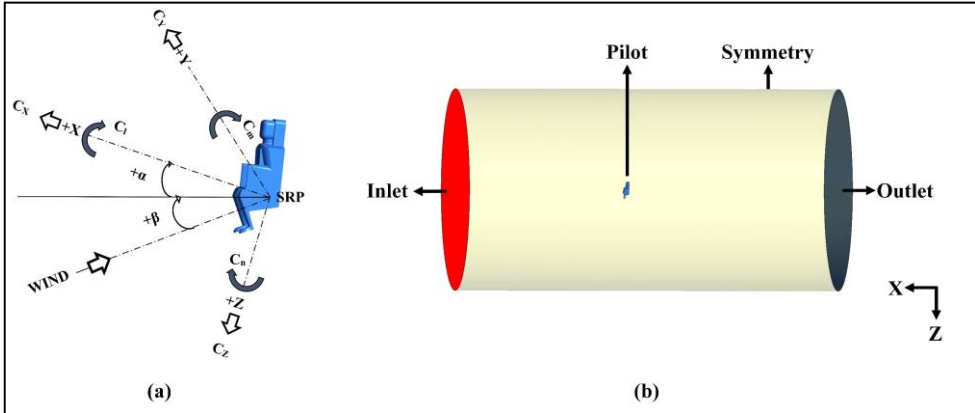
Very few literatures are available where the ejection seat system analyzed in the supersonic region. Hence, in this study, the ejection seat system is analyzed at Ma = 1.25 for different α to observe the aerodynamic characteristics. Before this study, no investigation was performed at this Ma. This influences the author to study a steady-state analysis on the ejection seat system at Ma = 1.25 for α = -15^0, -10^0, -5^0, 0^0, 5^0, 10^0, and 15^0. This investigation concludes that the changing of α has a significant consequence on the aerodynamic coefficients.

2 Methodology

2.1 Computational model and boundary conditions

For the analysis, a 3-D CAD model of the ejection seat system is prepared in SolidWorks. A simplified CAD model is prepared as the real model of the ejection seat system is complicated with sharp edges. The CAD model along with the aerodynamic coefficients and rotational angles is shown in Figure 1(a). The positive and the negative α generated when the model rotates clockwise and counterclockwise with respect to the Y-axis respectively. Air is used as the working fluid for the analysis where the density variation of the air is considered as the Ma of the working fluid is above 0.3.
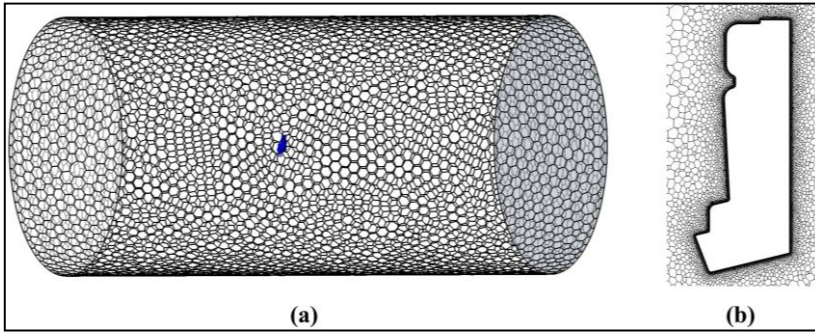
A cylindrical domain is prepared for this analysis where the far-field boundary condition is set at the inlet of the boundary and the pressure outlet is set at the outlet of the boundary. Symmetric condition is applied for the cylindrical surface and the surface of the ejection seat along with the occupant is assumed as a stationary wall with no-slip condition. Figure 1(b) depicts the boundary conditions used in this study.

Fig. 1. (a) Coordinate system with the aerodynamic coefficients, **(b)** boundary conditions.

2.2 Nnumerical computations

At the beginning of the grid generation, an unstructured grid with tetrahedron cells is created using ANSYS meshing software. Later on, the tetrahedron cells are converted into polyhedral cells in ANSYS Fluent shown in Figure 2. For this analysis around 15 inflation layer is created around the ejection seat system to resolve the viscous boundary layer.

Fig. 2. 3D Mesh model, **(a)** volume mesh, **(b)** close view of the mesh around the model.

A proper mesh independence study is performed for multiple mesh parameters at Ma = 0.6 and $\alpha = 0^0$ shown in Table 1.

Table 1. Grid Independence Study.

Mesh	Number of cells (million)	Cz (Numerical)	Cz (Experimental)
1	2.5	0.169	
2	3.5	0.161	
3	4.0	0.157	0.153
4	4.5	0.157	

From the table, it is observed that Mesh 3 is the ideal mesh that gives close results compared to the experimental result. With the greater number of grids, Mesh 4 generates outcomes which are similar to the Mesh 3. So, for further analysis of the ejection seat system, the parameters of the Mesh 3 are used.

2.3 Validation of the Numerical Approach

At Ma = 0.6, the numerical approaches are validated with the experimental results of White [1] by varying α from -15^0 to 15^0. To improve the accuracy second-order spatial discretization is utilized. The values of all the aerodynamic coefficients are obtained after the residual goes below 10^{-4}. Figure 3 displays the validation of the computed results with the experimental results where the computed and the experimental results match pretty well.
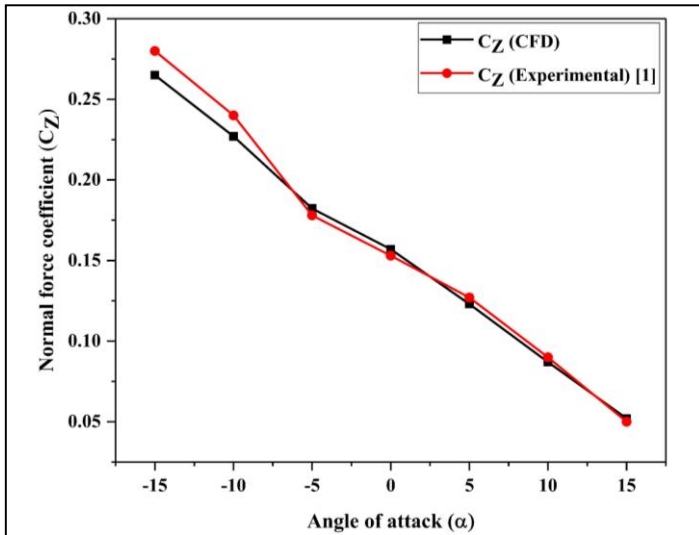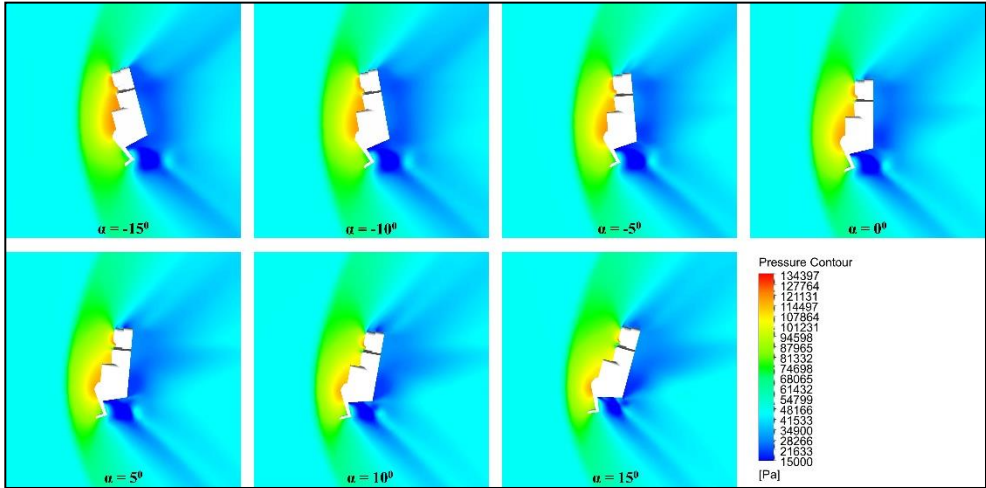

Fig. 3. Validation of the numerical methods.

3 Results and discussion

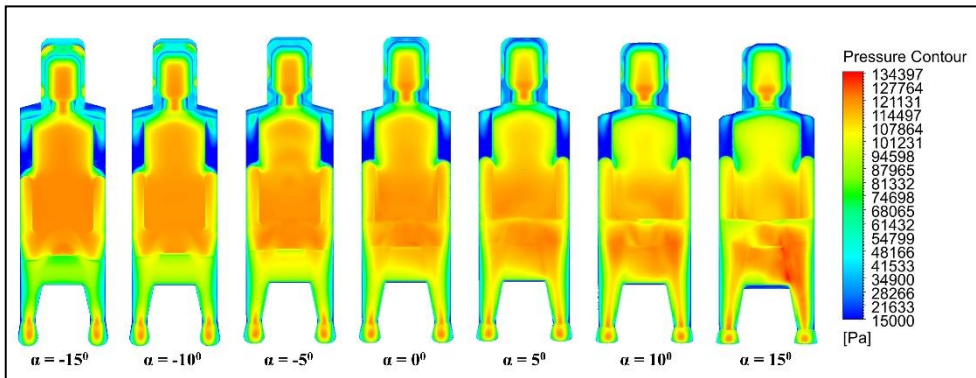### 3.1 Pressure distribution around the ejection seat system

Figure 4 shows the pressure contours on the symmetric plane of the ejection seat system at Ma = 1.25 for $\alpha = -15^0$, -10^0, -5^0, 0^0, 5^0, 10^0, and 15^0. From the figure it is observed that the maximum pressure region is at the front of the ejection seat system and the low pressure appears at the back of the ejection seat system. The intensity of the pressure changes as the α changes similarly the location of the high-pressure region changes as the α varies from -15^0 to 15^0. The flow separates due to the presence of the sharp edges in the ejection seat system which creates lower pressure at the back of the ejection seat system. An oblique shock appears at the front of the ejection seat system for all the α as the Ma of the free stream is 1.25.

Fig. 4. Pressure distribution on the symmetric plane at Ma = 1.25.

3.2 Aaerodynamic characteristics of the ejection seat system

Pressure contour on the pilot's surface at Ma = 1.25 for α = -15^0, -10^0, -5^0, 0^0, 5^0, 10^0, and 15^0 are shown in Figure 5. From the figure it is observed that the pressure on the pilot's surface changes with the α. At α = -15^0, the maximum pressure is found on the surface of the pilot. However, after α = -15^0, the intensity of the high pressure reduces with the increase of α.

Fig. 5. Pressure contour on the surface of the pilot at Ma = 1.25.

The magnitude of the C_X is increasing with the decrease of α which is shown in Figure 6. Due to the pressure difference between the front and rear surfaces, C_X is generated. The front surface of the pilot is largely exposed to the free stream at α = -15^0, compared to the other α. Due to the large exposed surface area, the magnitude of the C_X is maximum at this α which can be seen in Figure 5. After α = -15^0, the exposed surface area is reduced with the increase of α and eventually reduces the magnitude of the C_X. So, at α = -15^0 and 15^0, the maximum and minimum magnitude of the C_X is found.
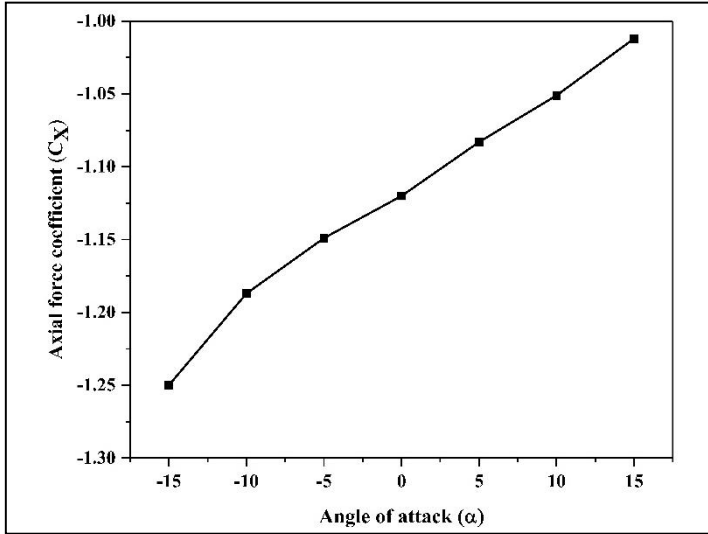
Fig. 6. Variation of C_X with the α at Ma = 1.25.

Figure 7(a) shows the variation of the C_Z with the α at Ma = 1.25. It can be observed that C_Z is inversely proportional to α. C_Z is generated due to the pressure difference between the top and bottom surfaces. With decreasing α, the higher pressure acting on the pilot's surface moves upward which creates a high-pressure difference and eventually increases the value of the C_Z. Hence, at $\alpha = -15^0$, the maximum value of the C_Z is found and at $\alpha = 15^0$, the minimum value of the C_Z is observed.

The variation of the C_m with the α at Ma = 1.25 is shown in Figure 7(b). Figure 7(b) depicts that the value of the C_m reduced with the increase of α. At $\alpha = -15^0$, the maximum value of the C_m is found whereas, at $\alpha = 15^0$, the minimum value of the C_m is observed.
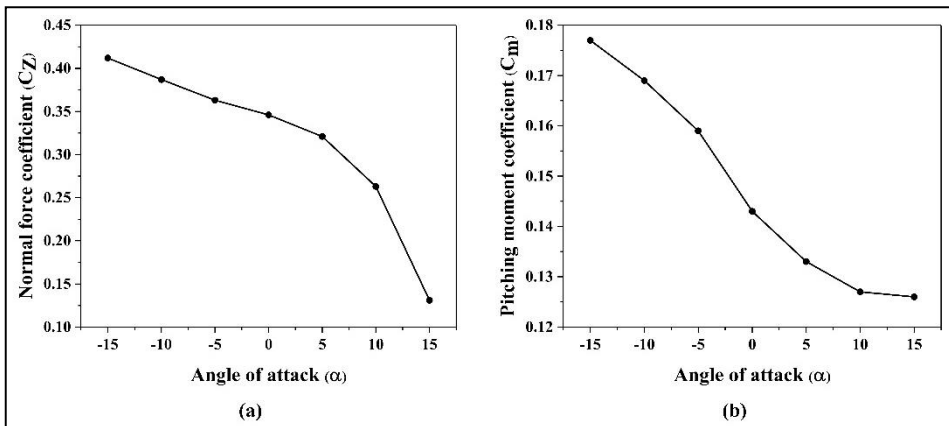

Fig. 7. (a) Variation of C_Z with the α at Ma = 1.25, **(b)** Variation of C_m with the α at Ma = 1.25.

4 Conclusions

In this study, the aerodynamic characteristics of a 3-D ejection seat system are analyzed using an unstructured grid in ANSYS-Fluent at Ma = 1.25 for $\alpha = -15^0$, -10^0, -5^0, 0^0, 5^0, 10^0, and 15^0 where the β remains at 0^0. The results obtained from this analysis are confirmed and demonstrate good agreement with the experimental data. The findings show that the pressure

acting on the surface of the pilot largely depends on the α. Similarly, the aerodynamic coefficients also change with the change of α which is summarized as follows,

  • The maximum pressure acting on the surface of the pilot is maximum at $\alpha = -15^0$, as the front surface of the pilot is largely exposed to the free stream and the intensity of the pressure is reduced as the α increases.

  • At $\alpha = -15^0$, the maximum magnitude of the C_X is found as the maximum pressure difference is observed and after that, the magnitude of the C_X is reduced as the α increases.

  • The minimum value of the C_Z is observed at $\alpha = 15^0$ due to less pressure difference between the top and bottom regions and the value of the C_Z is maximum at $\alpha = -15^0$.

  • The value of the C_m is found maximum at $\alpha = -15^0$ and the value of the C_m is found minimum at $\alpha = 15^0$.

  • The current study can be utilized while designing and developing an ejection seat system.

Acknowledgements

References

1. B. J. White, Aeromechanical properties of ejection seat escape systems, Air Force Flight Dynamics Lab Wright-Patterson AFB, OH., Apr. (1974)

2. Z. Wu, Z. Xie, P. Wang, W. Ding, Aerodynamic drag performance analysis of different types of high-speed train pantograph fairing. J. Appl. Sci. Eng. **23**, Issue 3, 509-519 (2020). DOI: 10.6180/jase.202009_23(3).0015

3. M. M. Rahman, A. K. M. Islam, Numerical study of convective heat transfer for turbulent flow in corrugated tube using Al2O3-water nanofluid, in AIP Conference Proceedings **2121**, Issue 1 (2019) DOI: 10.1063/1.5115916

4. S. S. Rajan, M. Santhoshkumar, N. Lakshmanan, N. S. Pillai, M. Paramasivam, CFD analysis and wind tunnel experiment on a typical launch vehicle model. J. Appl. Sci. Eng. **12**, Issue 3, 223-229 (2009). DOI: 10.6180/jase.2009.12.3.01

5. S. D. Habchi, A. J. Przekwas, T. Marquette, P. Ayoub, CFD analysis of ejection seat escape systems, SAE Transactions, 1566-1579 (1992) DOI: 10.4271/921924

6. S. Habchi, G. Hufford, Transient simulation of turbulent flow over blunt bodies (ejection seat configurations), in 13th Applied Aerodynamics Conference, Reston, Virigina: American Institute of Aeronautics and Astronautics, Jun. (1995) DOI: 10.2514/6.1995-1837

7. D. H. Chen, W. H. Wu, J. J. Wang, Y. Huang, Investigation on the aerodynamic performance of an ejection seat. Aeronaut. J. **111**, Issue 1120, 373–380 (2007). DOI: 10.1017/S0001924000004620

8. Y. Zhu, X. Zhao, S. Zhang, Computational studies of aircraft life-support systems, in 49th AIAA Aerospace Sciences Meeting including the New Horizons Forum and Aerospace Exposition, Reston, Virigina: American Institute of Aeronautics and Astronautics, Jan. (2011) DOI: 10.2514/6.2011-1045

9. J. L. Tian, L. Chen, Aerodynamic characteristics numerical simulation of the protective device of ejection seat. Appl. Mech. Mater. **229**, 1811–1814 (2012). DOI: 10.4028/www.scientific.net/AMM.229-231.1811

10. Y. Zhu, H. Guan, X. Zhao, S. Zhang, Computational studies of jettisoned canopy and ejection occupant/seat, in 50th AIAA Aerospace Sciences Meeting Including the New Horizons Forum and Aerospace Exposition (2012) DOI: 10.2514/6.2012-890

11. H. Guan, Y. Zhu, X. Zhao, S. Zhang, Aerodynamic characteristics of ejection seat and occupant, in 51st AIAA Aerospace Sciences Meeting including the New Horizons Forum and Aerospace Exposition, Reston, Virigina: American Institute of Aeronautics and Astronautics, Jan. (2013) DOI: 10.2514/6.2013-386

12. M. M. Rahman, V. Prakash, S. Chandel, D. G. Thakur, R. Čep, N. Khedkar, S. Salunkhe, E. S. Abouel Nasr, Analysis of the aerodynamic characteristics of an ejection seat system using computational fluid dynamics. Front. Mech. Eng. **9**, 1255051 (2023). DOI: 10.3389/fmech.2023.1255051